Mapping gains and losses in woody vegetation across global tropical drylands

Tian, Feng; Brandt, Martin Stefan; Liu, Yi Y; Rasmussen, Kjeld; Fensholt, Rasmus

Published in:
Global Change Biology

DOI:
10.1111/gcb.13464

Publication date:
2017

Document version
Peer reviewed version

Title: Mapping gains and losses in woody vegetation across global tropical drylands

Running head: Gains and losses in dryland woody vegetation

Authors: Feng Tian[1], Martin Brandt[1], Yi Y. Liu[2], Kjeld Rasmussen[1], Rasmus Fensholt[1]

[1] Department of Geosciences and Natural Resource Management, University of Copenhagen, 1350 Copenhagen, Denmark

[2] ARC Centre of Excellence for Climate Systems Science & Climate Change Research Centre, University of New South Wales, Sydney, Australia

Corresponding author: Feng Tian, Telephone: +45 35334738, emails: feng.tian@ign.ku.dk; ftian2012@gmail.com

Keywords: Trend analysis, non-photosynthetic woody component, drylands, woody vegetation, shrub encroachment, deforestation, remote sensing.

Type of Paper: Technical Advance

Abstract

Woody vegetation in global tropical drylands is of significant importance for both the inter-annual variability of the carbon cycle and local livelihoods. Satellite observations over the past decades provide a unique way to assess the vegetation long-term dynamics across biomes worldwide. Yet, the actual changes in the woody vegetation are always hidden by inter-annual fluctuations of the leaf density, because the most widely used remote sensing data are primarily related to the photosynthetically active vegetation components. Here, we quantify the temporal trends of the non-photosynthetic woody components (i.e. stems and branches) in global tropical drylands during 2000-2012 using the vegetation optical depth (VOD),

retrieved from passive microwave observations. This is achieved by a novel method focusing on the dry season period to minimize the influence of herbaceous vegetation, and using MODIS (MODerate resolution Imaging Spectroradiometer) NDVI (Normalized Difference Vegetation Index) data to remove the inter-annual fluctuation of the woody leaf component. We revealed significant trends ($p < 0.05$) in the woody component (VOD_{wood}) in 35% of the areas characterized by a non-significant NDVI trend, indicating pronounced gradual growth/decline in woody vegetation not captured by traditional assessments. The method is validated using a unique record of ground measurements from the semi-arid Sahel and shows a strong agreement between changes in VOD_{wood} and changes in ground observed woody cover ($r^2 = 0.78$). Reliability of the obtained woody component trends is also supported by a review of relevant literatures for eight hot-spot regions of change. The proposed approach is expected to contribute to an improved assessment of e.g. changes in dryland carbon pools.

Introduction

While vegetation in drylands has relatively low biomass, as compared to the humid areas, it is of significant importance for several reasons: Firstly, drylands cover approximately 41% of the Earth's terrestrial surface, and therefore total biomass and carbon stock of vegetation in drylands are still a substantial part of the global total (IPCC, 2014). Secondly, the variability of vegetation in drylands is comparatively high, implying that short-term changes in global carbon stocks may be dominated by the contribution from drylands (Ahlstrom *et al.*, 2015, Liu *et al.*, 2015). Thirdly, vegetation in drylands provides both products and services of great importance for local livelihoods (Adeel *et al.*, 2005). Trend analysis of long-term Earth Observation (EO) data has been widely used as means to assess vegetation dynamics in drylands (Fensholt *et al.*, 2012, Horion *et al.*, 2016). Moreover, different vegetation functional types (i.e. persistent vegetation and recurrent vegetation) have been assessed separately in

order to gain insights of the vegetation changes and its relation to changes in climate and human activities (Andela *et al.*, 2013, Archibald & Scholes, 2007, Donohue *et al.*, 2009, Fensholt *et al.*, 2015). Specifically, herbaceous vegetation is characterized by a short life-span (months or years) and large inter-annual variability driven by water availability and ecological disturbances (e.g. fires), whereas woody plants are characterized by a longer life-span (decades or centuries) with more stable growth conditions, particularly for the woody component (i.e. stems and branches).

Relatively few global scale quantitative studies on changes in dryland woody vegetation are available. Most researches on global deforestation/forest change are not designed to map woody vegetation in drylands, since they often do not fulfill the criteria of 'forest' (e.g. the FAO criterion of 10% crown cover, an area of more than 0.5 hectares and tree height above 5 m) (Hansen *et al.*, 2013, Shimada *et al.*, 2014). The few studies focusing on woody vegetation trends in drylands at regional scale used the normalized difference vegetation index (NDVI) data from optical sensors, e.g. MODerate resolution Imaging Spectroradiometer (MODIS) that are highly sensitive to the photosynthetic leaf component and largely insensitive to the non-photosynthetic woody component (Brandt *et al.*, 2016a, Horion *et al.*, 2014, Mitchard & Flintrop, 2013).

The leaf component is generally only a small fraction of the entire above-ground woody biomass, and may not be representative of the trends and spatial patterns of the woody component. In drylands the leaf component is often strongly related to water availability, and may therefore change quite rapidly depending on inter-annual variations in rainfall. Also, the spatial variability of soil conditions and topography partly control water availability. Moreover, large differences in phenology are found between woody species and consequently changes in species composition will result in substantial changes in the leaf component

72 (Brandt *et al.*, 2016b) that are not necessarily reflected in changes in woody biomass. In
73 addition, fires will have a considerable impact on inter-annual variations of leaf density and
74 mass. All these factors will cause inter-annual fluctuations of the leaf component and tend to
75 mask the supposedly more gradual and continuous trends in woody biomass.

76 Microwave sensor observations are sensitive to the water content in both photosynthetic
77 (herbaceous and woody plant leaves) and non-photosynthetic (woody stems and branches)
78 vegetation components (Jones *et al.*, 2013). The contribution of each component to the
79 observed signals highly depends on the microwave frequency used. Observations from low
80 frequency (i.e. 1.4 GHz) carry information mainly on the woody component (more related to
81 branches for forests), while the relative information on the leaf component increases
82 significantly with higher frequencies (Ferrazzoli *et al.*, 2002, Guglielmetti *et al.*, 2007, Santi
83 *et al.*, 2009). The L-band (1-2 GHz) radar backscatter has been shown to be highly correlated
84 to woody biomass in tropical savannas and woodlands (Mitchard *et al.*, 2009). Yet, available
85 L-band radar data have a limited record length hampering woody vegetation change studies
86 spanning decades, and it is still challenging to apply radar backscatter data for woody biomass
87 estimation at regional to global scales due to the difficulties of accounting for spatial
88 variability in soil properties and vegetation geometrical distributions at a high spatial
89 resolution (Kerr, 2007).

90 Recently, Liu *et al.* (2011) produced a global long-term vegetation optical depth (VOD)
91 dataset retrieved from satellite passive microwave radiometer observations at frequencies
92 higher than 6.8 GHz, which was shown to carry important information on woody vegetation
93 yet heavily influenced by the herbaceous vegetation and woody plant leaves (Grant *et al.*,
94 2016, Tian *et al.*, 2016). In this study, we present a method to separate the leaf and woody
95 components by the combined use of VOD and NDVI datasets to obtain a more accurate

assessment of woody vegetation changes/trends in global tropical drylands for the period 2000 to 2012.

Materials and methods

Study area

According to the UNEP (United Nations Environment Program) humidity map, global drylands are defined to include hyper-arid, arid, semi-arid and dry-subhumid regions. In this study, we focused on the tropical (between 35°N and 35°S) dryland areas, including the majority of woody vegetation of global drylands. Annual rainfall is usually below 800 mm and concentrated in the wet/growing season, with high inter-annual variability in both rainfall amount and timing (Adeel *et al.*, 2005). The typical vegetation in tropical drylands are annual herbaceous plants, shrubs and trees with open canopy cover, classified as savanna, shrublands or woodland depending on the dominant plant types. Annual herbaceous vegetation normally completes their life cycle during a single growing season spanning few months, governed by the timing of the rainy season. Contrastingly, trees and shrubs may show distinctly different seasonal cycles dependent on the species, i.e. evergreen, semi-evergreen or deciduous.

NDVI and VOD data

We used the Collection 6 Terra MODIS monthly product MOD13C2 with a spatial resolution of 0.05 degree (about 5.5 km at equator) and covering from 2000 to present (Didan, 2015). The surface reflectance bands have been corrected for atmospheric effects (Vermote & Kotchenova, 2008) and sensor degradation (Detsch *et al.*, 2016, Lyapustin *et al.*, 2014). To match the spatial resolution of VOD data, the red and near-infrared reflectance bands were aggregated to 0.25 degree by averaging before calculation of NDVI data.

The VOD data retrieval is based on the Land Parameter Retrieval Model (LPRM) (Owe *et al.*, 2001) with inputs of satellite passive microwave observations from several sensors, including the Special Sensor Microwave Imager (SSM/I), the Advanced Microwave Scanning Radiometer – Earth Observing System (AMSR-E), the WindSat and the FengYun-3B (Liu *et al.*, 2015). The microwave frequency of each sensor used is 19.4 GHz, 6.9 GHz, 6.8 GHz and 10 GHz, respectively. A cumulative distribution function (CDF) matching approach was used to merge the VOD retrievals from different sensors without changing the inter-annual variations and long-term trends (Liu *et al.*, 2012). The VOD dataset was produced at a monthly temporal interval from 1988 to 2012 and a spatial resolution of 0.25 degree (about 27 km at equator). The data is consistent among sensors as evaluated in Tian *et al.* (2016).

Conceptual design

The VOD retrievals from microwave emission at frequencies higher than 6.8 GHz are related to the water content in both the herbaceous plants and the woody plant leaves/stems/branches (Guglielmetti *et al.*, 2007, Santi *et al.*, 2009). In drylands characterized by a long dry season, the contribution from herbaceous vegetation will rapidly disappear and become negligible a few months into the dry season, and consequently the signal from woody vegetation will dominate. In order to separate the contributions from the leaf and woody components, we employed the independent information from MODIS NDVI which represents the amount of photosynthetically active plant material, and is largely determined by green leaves (i.e. leaf density) of woody vegetation in the dry season (Brandt *et al.*, 2016b). The overall conceptual design is shown in Fig. 1a and the detailed procedure of retrieving trends/changes in the woody component is described as follows (illustrated in supplementary material Fig. S1 based on simulated data):

i. For each pixel over a certain period of years, we decompose the observed dry season VOD (denoted as VOD_{raw}) and the corresponding observed NDVI signal (denoted as $NDVI_{raw}$) into two components: the long-term trend (LTT) and the inter-annual variations (IAV), respectively:

$$VOD_{raw} = VOD_{LTT} + \Delta VOD_{IAV} \quad (1)$$

$$NDVI_{raw} = NDVI_{LTT} + \Delta NDVI_{IAV} \quad (2)$$

Both the leaf and woody components would contribute to VOD_{LTT} and VOD_{IAV}, while the $NDVI_{LTT}$ and $NDVI_{IAV}$ are primarily attributed to the leaf component.

ii. If there is a significant correlation between VOD_{IAV} and $NDVI_{IAV}$, we assume that the VOD_{IAV} is dominated by a contribution from the leaf component while the woody component is relatively stable over time. Then we establish a linear regression between VOD_{IAV} and $NDVI_{IAV}$:

$$\Delta VOD_{IAV} = \beta \times \Delta NDVI_{IAV} + \varepsilon \quad (3)$$

Where β and ε are the slope and the residuals, respectively, varying as a function of woody vegetation density and species composition. Note that the intercept of the regression is 0 since both the independent and response variables have been already detrended. We built the regression model using the detrended VOD/NDVI instead of the original VOD/NDVI observations to avoid an underestimation of the trend in the woody component (Supplementary material Fig. S1).

iii. We apply the slope parameter (β) to $NDVI_{raw}$ to estimate the contribution from the leaf component to both VOD_{LTT} and VOD_{IAV} (denoted as VOD_{leaf}):

$$VOD_{leaf} = \beta \times NDVI_{raw} + b \quad (4)$$

Then the difference between VOD_{raw} and the estimated VOD_{leaf} would be the contribution from the woody component (denoted as VOD_{wood}):

$$VOD_{wood} = VOD_{raw} - VOD_{leaf} \quad (5)$$

It must be noted that we focus only on the long-term trends in VOD_{wood}, as the absolute values of VOD_{wood} cannot be obtained with the lack of estimation of b in equation (4).

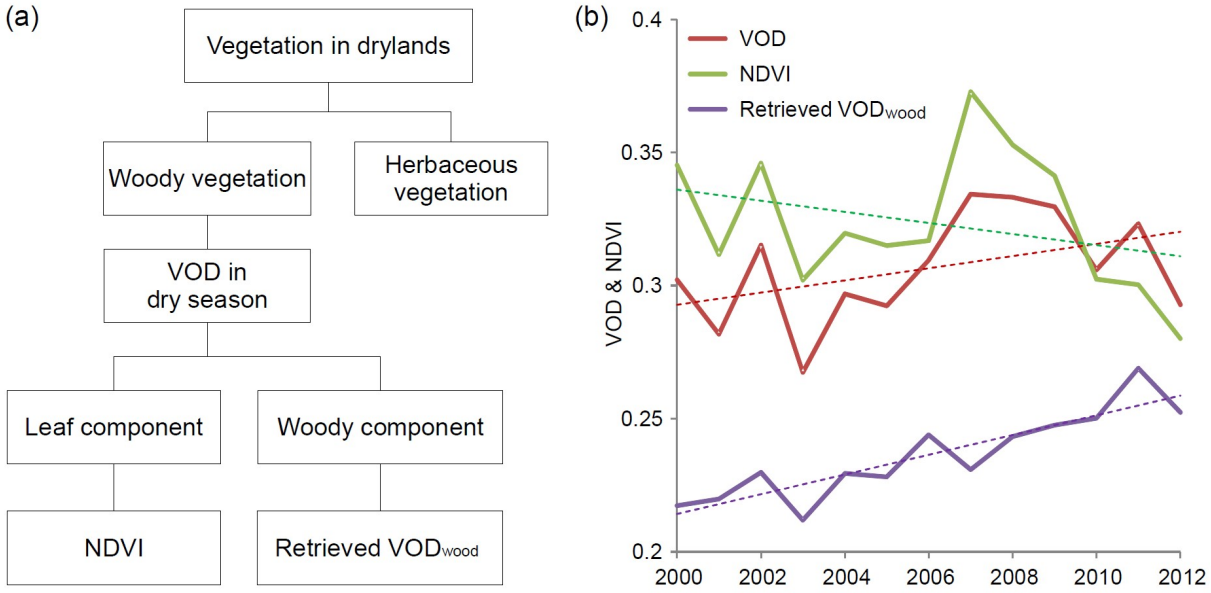

Fig. 1 (a) Conceptual design of the estimation of trends in the dryland woody vegetation component. (b) An example pixel (9.5°N, 18.75°E) showing the temporal profile of NDVI, VOD and the retrieved VOD_{wood}. Note that the focus of this approach is on the temporal trend of the retrieved VOD_{wood}, since the absolute values cannot be inferred.

Applying to remote sensing data

The method proposed was applied to monthly MODIS NDVI and VOD data from 2000 to 2012 being the intersection period of the NDVI and VOD datasets used. The VOD and NDVI data were detrended per pixel to obtain the inter-annual variation VOD_{IVA} and $NDVI_{IAV}$, respectively. Pixels with a non-significant t ($p \geq 0.05$) linear correlation between VOD_{IVA} and $NDVI_{IAV}$ were masked out for retrieval of VOD_{wood}, and also pixels with an NDVI value below 0.1 were excluded in the analysis to minimize influences from the soil background

(Huete, 1988). We determined the dry season period as the three months with lowest values in each dry season of the VOD observations (accounting for cross calendar-year minimum of VOD values in the southern hemisphere). To reduce the impact of cloud cover, we compared the Pearson product-moment correlation coefficient between all the seven possible combinations within the three months of detrended VOD and NDVI (i.e. first minimum, second minimum, third minimum, average of first and second minimum, average of first and third minimum, average of second and third minimum, and average of all the three months) and selected the one characterized by the highest r value. An example shows that the retrieved VOD_{wood} is more stable over time as compared to both NDVI and VOD (Fig. 1b). The NDVI trend was transformed into VOD units by multiplying the slope value β to be comparable with the retrieved VOD_{wood} trend.

Validation with in situ measurements

Time series data of *in situ* woody cover and leaf biomass available from Senegal were used to validate the retrieved trends of the woody and leaf components, respectively. Validating long-term trends requires continuous field data records covering a long time period and being representative for areas comparable with the spatial resolution of the satellite data. Moreover, *in situ* data should ideally include a broad range of ecosystem functional types and be located in areas where actual trends are observed. This study uses a unique data set of 11 ground sites (supplementary Fig. S2), located along a north-south rainfall gradient in Senegal (200-800 mm/year) covering the full time period of this study. The woody plant cover along this gradient increases from approximately 3% in the north to more than 40% in the south, including typical dryland evergreen and deciduous species (Brandt *et al.*, 2016b). Moreover, significant changes within the last 15 years are observed in these areas (Brandt *et al.*, 2015). Each site consists of a 1 km transect line, and the canopy cover of all woody plants

206 (regardless of size) was measured every two years in 4 circular plots, spaced at 200 m
207 intervals (Brandt *et al.*, 2016b). Furthermore, the leaf biomass of woody species was
208 investigated for the same sites using allometric models (Diouf *et al.*, 2015). Leaf mass and
209 density is closely related to inter-annual rainfall variations, whereas the woody cover is more
210 stable and representative for the woody vegetation density.

211 The scale differences between the *in situ* measurements and satellite data inevitably introduce
212 bias since pixel values generally tend to over/under estimate lowest/highest plot scale values
213 (Fensholt *et al.*, 2006). However, the sites are originally selected to be representative for
214 relatively large homogeneous areas (Diallo *et al.*, 1991) and have been successfully linked
215 with VOD pixels (Tian *et al*., 2016). Therefore, it was deemed feasible in this case to perform
216 pixel vs. plot scale comparisons between the trends of EO data and *in situ* measurements.

217 **Results**

218 ***Trends in different woody vegetation components***

219 The detrended dry season VOD data is significantly ($p < 0.05$) correlated with the
220 corresponding detrended NDVI data in 71% of global tropical drylands over the period 2000-
221 2012 (Fig. 2). For these areas, 14% of the NDVI pixels show significant trends ($p < 0.05$,
222 located mainly in southern Africa and Australia, Fig. 3b), while 27% of the VOD pixels have
223 significant trends (Fig. 3a). After removing the leaf inter-annual fluctuation from the VOD
224 signal, the retrieved VOD_{wood} shows significant trends in 36% of global tropical drylands (Fig.
225 3c). Furthermore, for pixels with a non-significant NDVI trend, 35% show a significant
226 VOD_{wood} trend (22% positive and 13% negative), revealing considerable areas characterized
227 by a woody vegetation trend obscured by leaf fluctuations (Fig. 4).

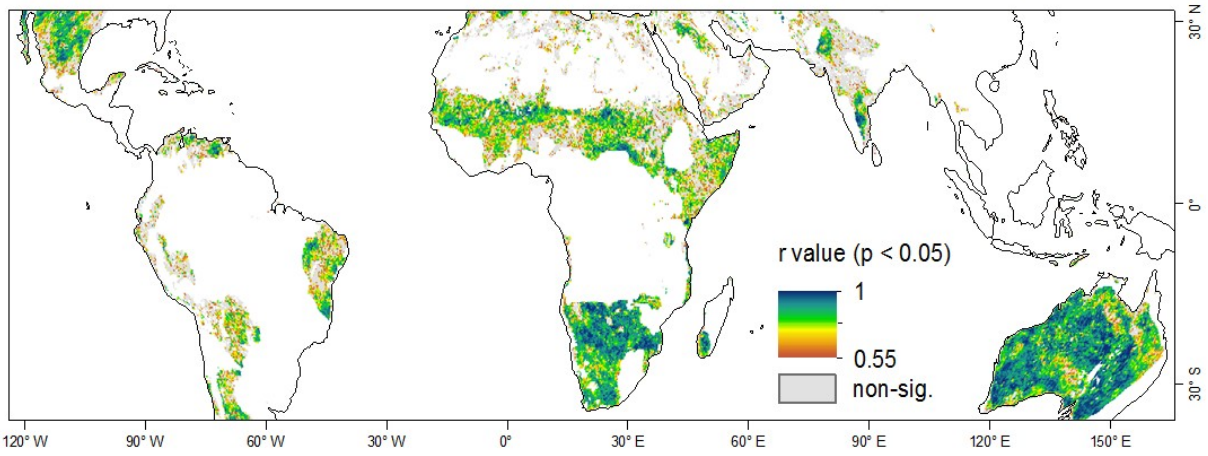

228

229 **Fig. 2** Correlation coefficients (r value) between detrended NDVI and detrended VOD time

230 series during 2000-2012.

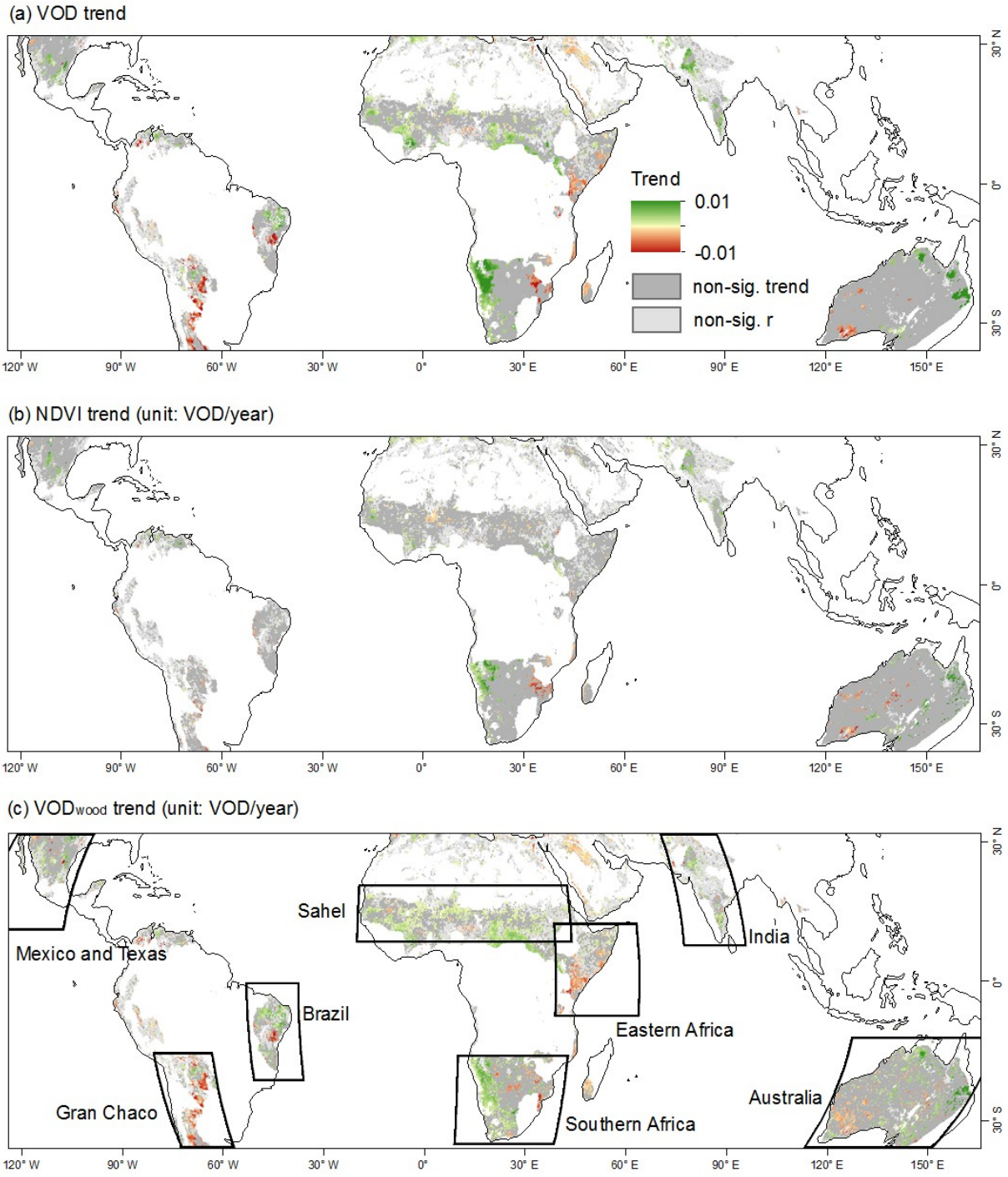

231

232 **Fig. 3** Trends of (a) VOD, (b) NDVI, and (c) VOD_{wood} during 2000-2012. Pixels with non-
233 significant ($p \geq 0.05$) correlation between detrended NDVI and detrended VOD are masked
234 with light grey color. Pixels with non-significant trends ($p \geq 0.05$) are masked with dark grey
235 color. Black boxes in (c) delineate hot-spot areas of VOD_{wood} changes (Fig. 6).

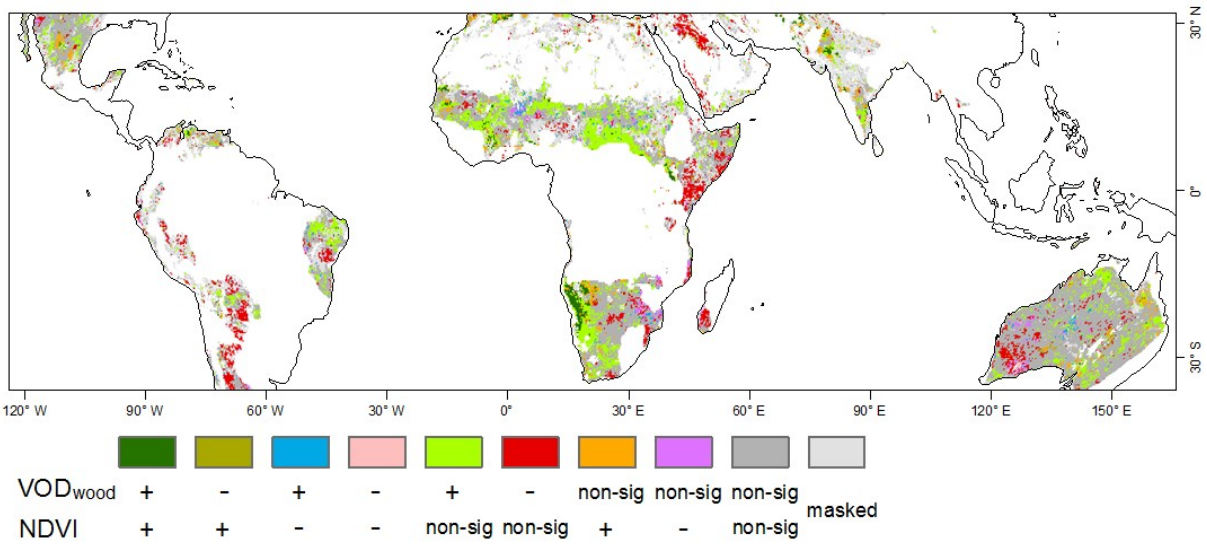

236

237 **Fig. 4** Spatial patterns of different trend combinations of VOD_{wood} (woody component) and
238 NDVI (leaf component).

239 ***Validation with in situ measurements***

240 The NDVI derived leaf trend is strongly coupled to the *in situ* leaf biomass trend ($r^2 = 0.59$; p
241 < 0.01, Fig. 5a), yet not significantly correlated with the *in situ* woody cover trend (Fig. 5c).
242 Contrastingly, the VOD_{wood} trend is highly correlated with the *in situ* woody cover trend ($r^2 =$
243 0.78; $p < 0.001$, Fig. 5f) whereas no significant correlation with the *in situ* leaf biomass trend
244 is observed (Fig. 5d). The VOD trend shows an intermediate correlation with both the *in situ*
245 leaf biomass trend ($r^2 = 0.27$; $p < 0.1$, Fig. 5b) and the *in situ* woody cover trend ($r^2 = 0.60$; p
246 < 0.01, Fig. 5e). Therefore, the method based on the complementary information in the VOD
247 and NDVI datasets has proven to successfully reduce the inter-annual fluctuations of the
248 VOD signal associated with the leaf component, thereby representing the woody vegetation
249 trend better than when using only VOD.

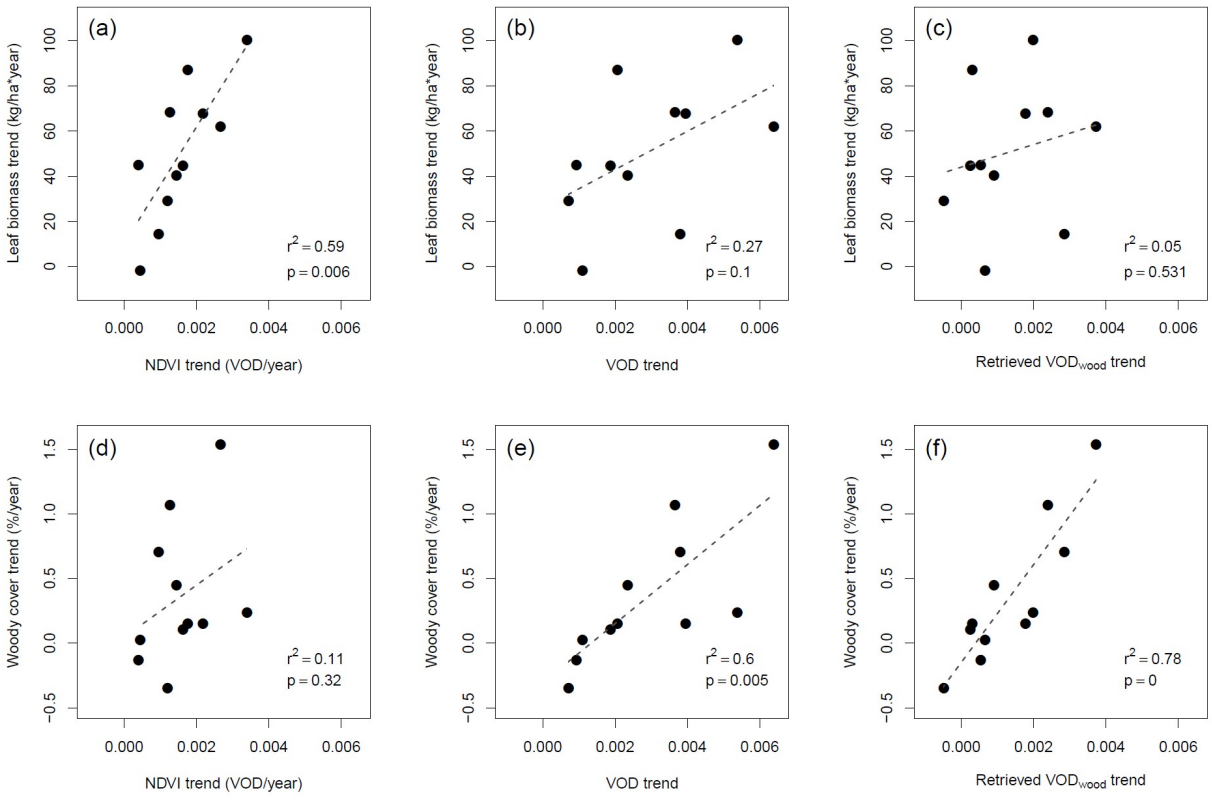

Fig. 5 Relationships between trends of *in situ* measured (a-c) leaf biomass and (d-f) woody canopy cover and trends of (a, d) NDVI, (b, e) VOD, and (c, f) VOD_{wood}. Locations and measurements of all *in situ* sites are shown in supplementary Fig. S2 and S3.

Sub-continental hot-spot regions of change

During the period 2000-2012, the trends in VOD_{wood} were found to be significantly ($p < 0.05$) positive in 22.7% of global tropical drylands whereas 13.3% were characterized by a significantly negative trend. We selected eight sub-continental hot-spot change regions of VOD_{wood} trends for further analyses (as indicated in Fig. 3c and enlarged in Fig. 6). The total area of significant VOD_{wood} trends and the percentage of significant trends per area for each hot-spot change region are summarized in Fig. 7. Large coherent areas of pronounced increasing VOD_{wood} trends are observed in Sahel, Namibia and South Africa, and East Australia. Contrastingly, areas of significant decreasing VOD_{wood} trends are found in Gran Chaco, eastern Africa, West Australia, and the eastern part of southern Africa.

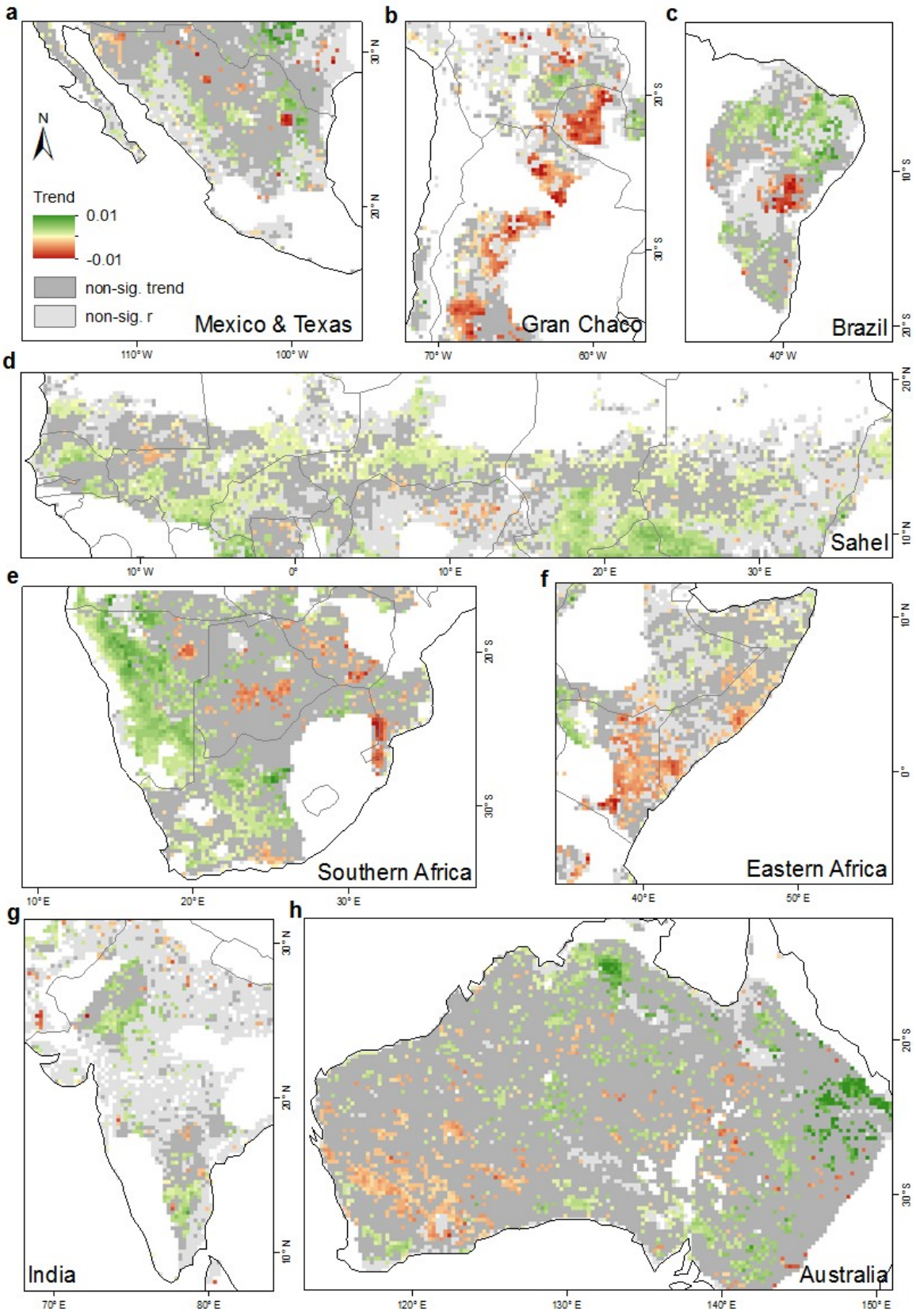

264

265 **Fig. 6** Trends of VOD_{wood} in hot-spot change regions of (a) Mexico & Texas, (b) Gran Chaco,

266 (c) Brazil, (d) Sahel, (e) southern Africa, (f) eastern Africa, (g) India, and (h) Australia.

Spatial extend of hot-spot change regions is indicated by the black boxes in Fig. 3c. Pixels with a non-significant ($p \geq 0.05$) correlation between detrended NDVI and detrended VOD are masked with light grey color. Pixels with non-significant trends ($p \geq 0.05$) are masked with dark grey color.

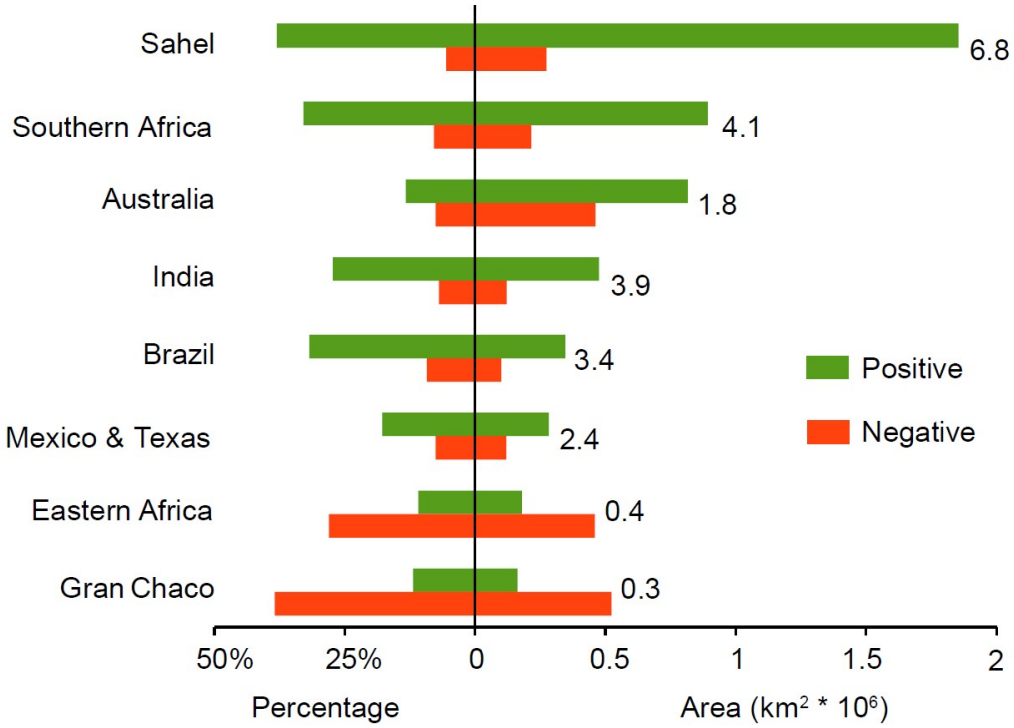

Fig. 7 Area (km^2*10^6) and percentages of significant ($p < 0.05$) positive and negative VOD_{wood} trends for the sub-continental hot-spot regions of change (Fig. 6). The ratio between areas of positive and negative trends is given by the number on the right side of each bar.

Discussion

Trends in woody vegetation

This study attained a separation between trends of the leaf and woody components in global tropical drylands (2000-2012) by combing satellite observations from optical and passive microwave sensors. By removing the inter-annual fluctuations and trends of the leaf component, we revealed regional scale trend patterns in woody vegetation which have not

been shown previously. In addition, we found areas characterized by diverging trends in the retrieved VOD_{wood} and NDVI data. This can be related to changes in composition of trees and shrubs within the footprint (~25 km) of a VOD pixel since trees and shrubs are characterized by different signatures in the proportion of leaf and woody components (Andela *et al.*, 2013). Given a similar amount of the woody component, shrubs generally look greener (higher NDVI) than trees as shrubs in this case will have a higher fractional vegetation cover. For example, Herrmann and Tappan (2013) reported an impoverishment of trees and encroachment of shrubs between the early 1980s and 2010 in central Senegal despite a positive NDVI trend. This area corresponds with the pixels with a non-significant VOD_{wood} trend and significant positive NDVI trend (colored as orange) in Fig. 4.

Quantifying trends/changes in different vegetation components remains a challenge for state-of-the-art dynamic global vegetation models (DGVMs) due to the complex responses of biomass partitioning process to plant type and size, nutrient supply and climate at global scale (De Kauwe *et al.*, 2014, Piao *et al.*, 2013, Poorter *et al.*, 2012). EO data provide measurements of land surface properties at global scale, allowing the assessment of vegetation dynamics directly (Liu *et al.*, 2015, Nemani *et al.*, 2003) and has also been coupled/compared with vegetation models (Calvet *et al.*, 2004, Poulter *et al.*, 2014). Yet, the most widely used EO data for EO/DGVM fusion is the optical satellite sensor vegetation index observations (NDVI) which are shown here to be unrelated to the non-photosynthetic woody vegetation component. This might be one of the reasons for the large discrepancy between the global terrestrial carbon storage estimated from DGVMs and EO data, respectively (Kolby Smith *et al.*, 2016). Therefore, if aiming at improved assessment of e.g. changes in dryland carbon pools or woody vegetation cover/mass changes (from EO data alone or assimilated into DGVMs), the presented method of combining EO optical and microwave remote sensing is expected to outperform the use of each of them separately.

306 ***Interpretation of sub-continental hot-spot regions of VOD_{wood} change***

307 The areas of increasing VOD_{wood} trends in Mexico and Texas, USA are likely related to shrub
308 encroachment mainly happening in the Chihuahuan Desert (Aide *et al.*, 2013, Van Auken,
309 2009), which was reported to be accelerating caused by a changing climatic conditions of
310 increasing temperatures (D'Odorico *et al.*, 2010). The significant decreasing VOD_{wood} trend in
311 the southeast of Texas corresponds well with the 2011 drought causing large scale tree
312 mortality as reported by Schwantes *et al.* (2016).

313 Extensive deforestation has taken place in vast parts of the Gran Chaco region characterized
314 by a transformation from dry deciduous forest into agriculture land (soybean production)
315 (Gasparri & Grau, 2009). These changes in land cover and land use (LULCC) were also
316 captured by medium/high resolution Landsat data (Hansen *et al.*, 2013). The VOD_{wood} trend
317 successfully detected this LULCC as a pronounced and widespread woody vegetation loss.

318 A return of woody vegetation in the Brazilian Caatinga region caused by the increases in
319 rainfall and decrease in the area under cultivation during 2001-2009 was reported by Redo *et*
320 *al.* (2013), which may explain the strongly positive VOD_{wood} trends in our analysis in
321 northeast part of Brazil. Contrastingly, decreasing VOD_{wood} trends in the south of Brazil
322 indicating a loss of woody vegetation, are likely to be caused by the highly degraded soil
323 conditions in this region (Almeida-Filho & Carvalho, 2010).

324 In the African Sahel, a greening trend driven by increasing rainfall after prolonged droughts
325 was reported using the AVHRR NDVI datasets (Herrmann *et al.*, 2005, Prince *et al.*, 2007).
326 However, this greening trend starting from early 1980s seems to have stabilized as assessed
327 using data from the MODIS sensor since 2000 (Horion *et al.*, 2014). This agrees well with the
328 NDVI based leaf component trend in this study (Fig. 3b). The widespread significant positive
329 VOD_{wood} trends (Fig. 6d) indicate that the density of woody vegetation stands have continued

to increase during 2000-2012, which is in line with the findings of Brandt *et al.* (2016a). Besides the overall increasing trend, losses of woody vegetation are also seen in the Sahel e.g. northern Nigeria which was reported to be caused by logging and agricultural expansion into forest reserves (Brandt *et al.*, 2016a).

The extensive shrub encroachment in the drylands of Namibia and South Africa (Buitenwerf *et al.*, 2012, O'Connor *et al.*, 2014, Rohde & Hoffman, 2012) is supported by the significant positive trends in both the NDVI based leaf component and retrieved VOD_{wood} based woody component. However, the VOD_{wood} shows much larger areas of positive trends as compared to NDVI (Fig. 4), indicating a potential under-estimation of the spatial extent of shrub encroachment based on optical remote sensing data in this region (Saha *et al.*, 2015). Manmade fires are used for controlling bush encroachment in Botswana and Zimbabwe (Gandiwa, 2011, Mudongo *et al.*, 2016). While fire rarely kill trees, bush encroachment is suppressed and ultimately will lead to a reduction in the size of woody plants (Higgins *et al.*, 2007). Therefore, an intensification of fire events during this period as observed by Andela and van der Werf (2014) would be a plausible explanation for the overall decreasing VOD_{wood} trends in Botswana and Zimbabwe.

Selective logging of hardwood trees species for charcoal production was reported to introduce land degradation in the woodland regions of Kenya (Ndegwa *et al.*, 2016). Also, massive logging and deforestation for charcoal and livestock production is happening in Somalia (Oduori *et al.*, 2011, Rembold *et al.*, 2013) which together may explain the widespread pattern of decreasing VOD_{wood} trends in East Africa (Fig. 6f).

A consistent increasing trend was observed in the retrieved VOD_{wood} for India, meaning an increase in the forest cover or natural growth of trees during the period studied. This may be

attributed to the large scale implementation of policies aiming at developing forest protection programs (Reddy *et al.*, 2013, Tian *et al.*, 2014).

The geographical patterns of VOD_{wood} trends in Australia correspond well with the substantial changes in water availability during the period studied (Xie *et al.*, 2016). A continues decline in water storage was reported in Australia during the early 21st-century caused by long lasting droughts (known as the 'big dry'), being particularly severe in the southwestern part causing widespread tree mortality (Brouwers *et al.*, 2013, McGrath *et al.*, 2012). Effects of water loss were compensated or even reversed by a continental-scale water gain in 2010 and 2011, particularly strong in the eastern part (Xie *et al.*, 2016).

Limitations and Outlook

The microwave observations used in this long-term VOD dataset cannot always penetrate the entire vegetation layer (e.g. rainforest). To mitigate this potential limitation of the usage of VOD, our study focuses on dryland areas only. Since we are aiming to detect changes in the woody component, herbaceous and crops would perturb the estimation accuracy due to their different relationships with satellite observations as compared to woody vegetation (Tian *et al.*, 2016). The use of VOD observations from only the dry season facilitates accurate detection of the water content in woody component, but remnants of senescent material from leftover herbaceous vegetation and crops, together with soil background, may still introduce noise. However, a significant relationship between VOD and NDVI time series would ensure that the impacts of error sources on the estimated trends remain at a low level.

VOD is reported to be linearly related to the vegetation water content in green vegetation component, depending on vegetation structure, microwave frequency, and vegetation water status (Griend & Wigneron, 2004, Jackson & Schmugge, 1991, Wigneron *et al.*, 2004). Yet, the relationship between VOD and vegetation water content in the woody component may be

more complex considering the varying sizes, heights, shapes and species of woody plants (Jones *et al.*, 2011). Furthermore, the relationship between water content/VOD and woody biomass is also expected to be more complex, which may change with the soil conditions and woody species composition (Sternberg & Shoshany, 2001). In combination with a lack of ground observations, these potentially confounding factors made it difficult to transform VOD_{wood} to the units of biomass.

The AVHRR sensors have observations since early 1980s, forming the basis for global long-term NDVI datasets. Yet, several problems made it challenging to merge observations from difference sensors in a temporally consistent way (Tian *et al.*, 2015), especially during the dry season (Horion *et al.*, 2014). As for the passive microwave records, although differences of the microwave frequencies exist between sensors (e.g. 19.4 GHz for SSM/I and 6.9GHz for AMSR-E), the sensitivity of observed microwave emissions to the leaf component was reported to be similar at these frequencies (Santi *et al.*, 2009). Moreover, the long overlapping period between different sensors made it possible to calibrate VOD retrievals successfully (Liu *et al.*, 2011). Consequently, the availability of an improved AVHRR based long-term NDVI products (expected release in the near future) will extend the analysis period of woody component trends to around three decades.

Recently, several passive microwave satellite instruments operating at L-band (1.4 GHz) have been launched, i.e. the Soil Moisture and Ocean Salinity (SMOS, 2010 - present), the Aquarius (2011 - 2015) and the Soil Moisture Active Passive (SMAP). As the leaf component is close to be transparent at L-band (Guglielmetti *et al.*, 2007, Santi *et al.*, 2009), observations from these sensors are expected to be more directly linked to information on the woody component (Grant *et al.*, 2016, Vittucci *et al.*, 2016). Due to their short time period of operation, trend analyses on these L-band observations are not yet feasible. However, with

observations continued in the near future, temporal trends of VOD retrievals from SMOS and SMAP can be compared with the trends of the approach developed in this study. If promising, they can be merged into a long-term time series to assist analyzing changes in woody vegetation.

Acknowledgements

This research is partly funded by the China Scholarship Council (CSC, number 201306420005) and the Danish Council for Independent Research (DFF) Sapere Aude programme under the project entitled "Earth Observation based Vegetation productivity and Land Degradation Trends in Global Drylands". M. B. is the recipient of the European Union's Horizon 2020 research and innovation programme under the Marie Sklodowska-Curie grant agreement (project number 656564). Y.Y.L. is the recipient of an Australian Research Council Discovery Early Career Researcher Award (DECRA) Fellowship (project number DE140100200). We thank the Centre de Suivi Ecologique (Senegal) and especially Abdoulaye Wele and Abdoul Aziz Diouf for collecting and providing the field data on woody cover and leaf biomass, and Neha Joshi, University of Copenhagen for helpful discussions on the properties of passive microwave and radar observations.

References

Adeel Z, Safriel U, Niemeijer D *et al.* (2005) *Ecosystems and human well-being: desertification synthesis. A Report of the Millennium Ecosystem Assessment,* Washington, DC, World Resources Institute.

Ahlstrom A, Raupach MR, Schurgers G *et al.* (2015) The dominant role of semi-arid ecosystems in the trend and variability of the land CO2 sink. Science*,* **348**, 895-899.

Aide TM, Clark ML, Grau HR *et al.* (2013) Deforestation and Reforestation of Latin America and the Caribbean (2001–2010). Biotropica*,* **45**, 262-271.

Almeida-Filho R, Carvalho CM (2010) Mapping land degradation in the Gilbués region, northeastern Brazil, using Landsat TM images. International Journal of Remote Sensing, **31**, 1087-1094.
Andela N, Liu YY, Van Dijk AIJM, De Jeu RaM, Mcvicar TR (2013) Global changes in dryland vegetation dynamics (1988-2008) assessed by satellite remote sensing: comparing a new passive microwave vegetation density record with reflective greenness data. Biogeosciences, **10**, 6657-6676.
Andela N, Van Der Werf GR (2014) Recent trends in African fires driven by cropland expansion and El Nino to La Nina transition. Nature Climate Change, **4**, 791-795.
Archibald S, Scholes RJ (2007) Leaf green-up in a semi-arid African savanna -separating tree and grass responses to environmental cues. Journal of Vegetation Science, **18**, 583-594.
Brandt M, Hiernaux P, Rasmussen K *et al.* (2016a) Assessing woody vegetation trends in Sahelian drylands using MODIS based seasonal metrics. Remote Sensing of Environment, **183**, 215-225.
Brandt M, Hiernaux P, Tagesson T *et al.* (2016b) Woody plant cover estimation in drylands from Earth Observation based seasonal metrics. Remote Sensing of Environment, **172**, 28-38.
Brandt M, Mbow C, Diouf AA, Verger A, Samimi C, Fensholt R (2015) Ground- and satellite-based evidence of the biophysical mechanisms behind the greening Sahel. Global Change Biology, 1610-1620.
Brouwers NC, Mercer J, Lyons T, Poot P, Veneklaas E, Hardy G (2013) Climate and landscape drivers of tree decline in a Mediterranean ecoregion. Ecology and Evolution, **3**, 67-79.
Buitenwerf R, Bond WJ, Stevens N, Trollope WSW (2012) Increased tree densities in South African savannas: >50 years of data suggests CO2 as a driver. Global Change Biology, **18**, 675-684.
Calvet JC, Viterbo P, Ciais P *et al.* (2004) Assimilation of remote sensing data to monitor the terrestrial carbon cycle: The carbon observatory of geoland. In: *Geoscience and Remote Sensing Symposium, 2004. IGARSS '04. Proceedings. 2004 IEEE International.* pp Page.
D'odorico P, Fuentes JD, Pockman WT *et al.* (2010) Positive feedback between microclimate and shrub encroachment in the northern Chihuahuan desert. Ecosphere, **1**, 1-11.
De Kauwe MG, Medlyn BE, Zaehle S *et al.* (2014) Where does the carbon go? A model–data intercomparison of vegetation carbon allocation and turnover processes at two temperate forest free-air CO2 enrichment sites. New Phytologist, **203**, 883-899.
Detsch F, Otte I, Appelhans T, Nauss T (2016) A Comparative Study of Cross-Product NDVI Dynamics in the Kilimanjaro Region—A Matter of Sensor, Degradation Calibration, and Significance. Remote Sensing, **8**, 159.
Diallo O, Diouf A, Hanan NP, Ndiaye A, Prévost Y (1991) AVHRR monitoring of savanna primary production in Senegal, West Africa: 1987-1988. International Journal of Remote Sensing, **12**, 1259-1279.
Didan K (2015) MOD13C2 MODIS/Terra Vegetation Indices Monthly L3 Global 0.05Deg CMG V006. NASA EOSDIS Land Processes DAAC. Retrieved from http://dx.doi.org/10.5067/MODIS/MOD13C2.006.
Diouf A, Brandt M, Verger A *et al.* (2015) Fodder Biomass Monitoring in Sahelian Rangelands Using Phenological Metrics from FAPAR Time Series. Remote Sensing, **7**, 9122.
Donohue RJ, Mcvicar TR, Roderick ML (2009) Climate-related trends in Australian vegetation cover as inferred from satellite observations, 1981–2006. Global Change Biology, **15**, 1025-1039.
Fensholt R, Horion S, Tagesson T, Ehammer A, Ivits E, Rasmussen K (2015) Global-scale mapping of changes in ecosystem functioning from earth observation-based trends in total and recurrent vegetation. Global Ecology and Biogeography, **24**, 1003-1017.
Fensholt R, Langanke T, Rasmussen K *et al.* (2012) Greenness in semi-arid areas across the globe 1981–2007 — an Earth Observing Satellite based analysis of trends and drivers. Remote Sensing of Environment, **121**, 144-158.
Fensholt R, Sandholt I, Rasmussen MS, Stisen S, Diouf A (2006) Evaluation of satellite based primary production modelling in the semi-arid Sahel. Remote Sensing of Environment, **105**, 173-188.
Ferrazzoli P, Guerriero L, Wigneron JP (2002) Simulating L-band emission of forests in view of future satellite applications. Ieee Transactions on Geoscience and Remote Sensing, **40**, 2700-2708.
Gandiwa E (2011) Effects of repeated burning on woody vegetation structure and composition in a semiarid southern African savanna. International journal of environmental sciences, **2**, 458.
Gasparri NI, Grau HR (2009) Deforestation and fragmentation of Chaco dry forest in NW Argentina (1972–2007). Forest Ecology and Management, **258**, 913-921.

Grant JP, Wigneron JP, De Jeu RaM *et al.* (2016) Comparison of SMOS and AMSR-E vegetation optical depth to four MODIS-based vegetation indices. Remote Sensing of Environment, **172**, 87-100.
Griend AaVD, Wigneron JP (2004) The b-factor as a function of frequency and canopy type at H-polarization. Ieee Transactions on Geoscience and Remote Sensing, **42**, 786-794.
Guglielmetti M, Schwank M, Mätzler C, Oberdörster C, Vanderborght J, Flühler H (2007) Measured microwave radiative transfer properties of a deciduous forest canopy. Remote Sensing of Environment, **109**, 523-532.
Hansen MC, Potapov PV, Moore R *et al.* (2013) High-Resolution Global Maps of 21st-Century Forest Cover Change. Science, **342**, 850-853.
Herrmann SM, Anyamba A, Tucker CJ (2005) Recent trends in vegetation dynamics in the African Sahel and their relationship to climate. Global Environmental Change, **15**, 394-404.
Herrmann SM, Tappan GG (2013) Vegetation impoverishment despite greening: A case study from central Senegal. Journal of Arid Environments, **90**, 55-66.
Higgins SI, Bond WJ, February EC *et al.* (2007) Effects of four decades of fire manipulation on woody vegetation structure in savanna. Ecology, **88**, 1119-1125.
Horion S, Fensholt R, Tagesson T, Ehammer A (2014) Using earth observation-based dry season NDVI trends for assessment of changes in tree cover in the Sahel. International Journal of Remote Sensing, **35**, 2493-2515.
Horion S, Prishchepov AV, Verbesselt J, De Beurs K, Tagesson T, Fensholt R (2016) Revealing turning points in ecosystem functioning over the Northern Eurasian agricultural frontier. Global Change Biology, n/a-n/a.
Huete AR (1988) A soil-adjusted vegetation index (SAVI). Remote Sensing of Environment, **25**, 295-309.
Ipcc (2014) Climate Change 2014: Synthesis Report. Contribution of Working Groups I, II and III to the Fifth Assessment Report of the Intergovernmental Panel on Climate Change [Core Writing Team, R.K. Pachauri and L.A. Meyer (eds.)]. IPCC, Geneva, Switzerland, 151 pp.
Jackson TJ, Schmugge TJ (1991) Vegetation effects on the microwave emission of soils. Remote Sensing of Environment, **36**, 203-212.
Jones MO, Jones LA, Kimball JS, Mcdonald KC (2011) Satellite passive microwave remote sensing for monitoring global land surface phenology. Remote Sensing of Environment, **115**, 1102-1114.
Jones MO, Kimball JS, Jones LA (2013) Satellite microwave detection of boreal forest recovery from the extreme 2004 wildfires in Alaska and Canada. Global Change Biology, **19**, 3111-3122.
Kerr YH (2007) Soil moisture from space: Where are we? Hydrogeology Journal, **15**, 117-120.
Kolby Smith W, Reed SC, Cleveland CC *et al.* (2016) Large divergence of satellite and Earth system model estimates of global terrestrial CO2 fertilization. Nature Clim. Change, **6**, 306-310.
Liu YY, De Jeu RaM, Mccabe MF, Evans JP, Van Dijk AIJM (2011) Global long-term passive microwave satellite-based retrievals of vegetation optical depth. Geophysical Research Letters, **38**.
Liu YY, Dorigo WA, Parinussa RM *et al.* (2012) Trend-preserving blending of passive and active microwave soil moisture retrievals. Remote Sensing of Environment, **123**, 280-297.
Liu YY, Van Dijk AIJM, De Jeu RaM, Canadell JG, Mccabe MF, Evans JP, Wang G (2015) Recent reversal in loss of global terrestrial biomass. Nature Climate Change, **5**, 470-474.
Lyapustin A, Wang Y, Xiong X *et al.* (2014) Scientific impact of MODIS C5 calibration degradation and C6+ improvements. Atmospheric Measurement Techniques, **7**, 4353-4365.
Mcgrath GS, Sadler R, Fleming K, Tregoning P, Hinz C, Veneklaas EJ (2012) Tropical cyclones and the ecohydrology of Australia's recent continental-scale drought. Geophysical Research Letters, **39**, n/a-n/a.
Mitchard ETA, Flintrop CM (2013) Woody encroachment and forest degradation in sub-Saharan Africa's woodlands and savannas 1982–2006. Philosophical Transactions of the Royal Society of London B: Biological Sciences, **368**.
Mitchard ETA, Saatchi SS, Woodhouse IH *et al.* (2009) Using satellite radar backscatter to predict above-ground woody biomass: A consistent relationship across four different African landscapes. Geophysical Research Letters, **36**, n/a-n/a.
Mudongo E, Fynn R, Bonyongo MC (2016) Influence of fire on woody vegetation density, cover and structure at Tiisa Kalahari Ranch in western Botswana. Grassland Science, **62**, 3-11.

Ndegwa GM, Nehren U, Grüninger F, Iiyama M, Anhuf D (2016) Charcoal production through selective logging leads to degradation of dry woodlands: a case study from Mutomo District, Kenya. Journal of Arid Land, **8**, 618-631.
Nemani RR, Keeling CD, Hashimoto H *et al.* (2003) Climate-Driven Increases in Global Terrestrial Net Primary Production from 1982 to 1999. Science, **300**, 1560-1563.
O'connor TG, Puttick JR, Hoffman MT (2014) Bush encroachment in southern Africa: changes and causes. African Journal of Range & Forage Science, **31**, 67-88.
Oduori SM, Rembold F, Abdulle OH, Vargas R (2011) Assessment of charcoal driven deforestation rates in a fragile rangeland environment in North Eastern Somalia using very high resolution imagery. Journal of Arid Environments, **75**, 1173-1181.
Owe M, De Jeu R, Walker J (2001) A methodology for surface soil moisture and vegetation optical depth retrieval using the microwave polarization difference index. Ieee Transactions on Geoscience and Remote Sensing, **39**, 1643-1654.
Piao S, Sitch S, Ciais P *et al.* (2013) Evaluation of terrestrial carbon cycle models for their response to climate variability and to CO2 trends. Global Change Biology, **19**, 2117-2132.
Poorter H, Niklas KJ, Reich PB, Oleksyn J, Poot P, Mommer L (2012) Biomass allocation to leaves, stems and roots: meta-analyses of interspecific variation and environmental control. New Phytologist, **193**, 30-50.
Poulter B, Frank D, Ciais P *et al.* (2014) Contribution of semi-arid ecosystems to interannual variability of the global carbon cycle. Nature, **509**, 600-603.
Prince SD, Wessels KJ, Tucker CJ, Nicholson SE (2007) Desertification in the Sahel: a reinterpretation of a reinterpretation. Global Change Biology, **13**, 1308-1313.
Reddy CS, Dutta K, Jha CS (2013) Analysing the gross and net deforestation rates in India. Current Science, **105**, 1492-1500.
Redo D, Aide TM, Clark ML (2013) Vegetation change in Brazil's dryland ecoregions and the relationship to crop production and environmental factors: Cerrado, Caatinga, and Mato Grosso, 2001–2009. Journal of Land Use Science, **8**, 123-153.
Rembold F, Oduori SM, Gadain H, Toselli P (2013) Mapping charcoal driven forest degradation during the main period of Al Shabaab control in Southern Somalia. Energy for Sustainable Development, **17**, 510-514.
Rohde RF, Hoffman MT (2012) The historical ecology of Namibian rangelands: Vegetation change since 1876 in response to local and global drivers. Science of The Total Environment, **416**, 276-288.
Saha MV, Scanlon TM, D'odorico P (2015) Examining the linkage between shrub encroachment and recent greening in water-limited southern Africa. Ecosphere, **6**, 1-16.
Santi E, Paloscia S, Pampaloni P, Pettinato S (2009) Ground-Based Microwave Investigations of Forest Plots in Italy. Ieee Transactions on Geoscience and Remote Sensing, **47**, 3016-3025.
Schwantes AM, Swenson JJ, Jackson RB (2016) Quantifying drought-induced tree mortality in the open canopy woodlands of central Texas. Remote Sensing of Environment, **181**, 54-64.
Shimada M, Itoh T, Motooka T, Watanabe M, Shiraishi T, Thapa R, Lucas R (2014) New global forest/non-forest maps from ALOS PALSAR data (2007–2010). Remote Sensing of Environment, **155**, 13-31.
Sternberg M, Shoshany M (2001) Aboveground biomass allocation and water content relationships in Mediterranean trees and shrubs in two climatological regions in Israel. Plant Ecology, **157**, 173-181.
Tian F, Brandt M, Liu YY *et al.* (2016) Remote sensing of vegetation dynamics in drylands: Evaluating vegetation optical depth (VOD) using AVHRR NDVI and in situ green biomass data over West African Sahel. Remote Sensing of Environment, **177**, 265-276.
Tian F, Fensholt R, Verbesselt J, Grogan K, Horion S, Wang Y (2015) Evaluating temporal consistency of long-term global NDVI datasets for trend analysis. Remote Sensing of Environment, **163**, 326-340.
Tian H, Banger K, Bo T, Dadhwal VK (2014) History of land use in India during 1880–2010: Large-scale land transformations reconstructed from satellite data and historical archives. Global and Planetary Change, **121**, 78-88.
Van Auken OW (2009) Causes and consequences of woody plant encroachment into western North American grasslands. Journal of Environmental Management, **90**, 2931-2942.
Vermote EF, Kotchenova S (2008) Atmospheric correction for the monitoring of land surfaces. Journal of Geophysical Research: Atmospheres, **113**, 1-12.

600 Vittucci C, Ferrazzoli P, Kerr Y, Richaume P, Guerriero L, Rahmoune R, Laurin GV (2016) SMOS
601 retrieval over forests: Exploitation of optical depth and tests of soil moisture estimates.
602 Remote Sensing of Environment, **180**, 115-127.
603 Wigneron J-P, Kerr Y, Chanzy A, Jin Y-Q (1993) Inversion of surface parameters from passive
604 microwave measurements over a soybean field. Remote Sensing of Environment, **46**, 61-72.
605 Wigneron JP, Parde M, Waldteufel P, Chanzy A, Kerr Y, Schmidl S, Skou N (2004) Characterizing
606 the dependence of vegetation model parameters on crop structure, incidence angle, and
607 polarization at L-band. Ieee Transactions on Geoscience and Remote Sensing, **42**, 416-425.
608 Xie Z, Huete A, Restrepo-Coupe N, Ma X, Devadas R, Caprarelli G (2016) Spatial partitioning and
609 temporal evolution of Australia's total water storage under extreme hydroclimatic impacts.
610 Remote Sensing of Environment, **183**, 43-52.

611

Supporting Information captions

Fig. S1. Example of the conceptual design based on simulated data.

Fig. S2. Location of the *in situ* sites.

Fig. S3. *In situ* measurements of leaf biomass and woody cover data.